27 May 2007

# Final report for EOARD grant FA8655-07-1-3059

"Improvement of electromagnetic code
for phased array antenna design"

Dr. Henrik Holter

# REPORT DOCUMENTATION PAGE

Form Approved OMB No. 0704-0188



| 1. REPORT DATE *(DD-MM-YYYY)* | 2. REPORT TYPE | 3. DATES COVERED *(From – To)* |
|---|---|---|
| 01-06-2007 | Final Report | 1 March 2007 - 01-Sep-07 |

**4. TITLE AND SUBTITLE**

Improvement of electromagnetic code for phased array antenna design

**5a. CONTRACT NUMBER**
FA8655-07-1-3059

**5b. GRANT NUMBER**

**5c. PROGRAM ELEMENT NUMBER**

**6. AUTHOR(S)**

Dr. Henrik P Holter

**5d. PROJECT NUMBER**

**5d. TASK NUMBER**

**5e. WORK UNIT NUMBER**

**7. PERFORMING ORGANIZATION NAME(S) AND ADDRESS(ES)**
Henrik P Holter
Korsuddsvagen 17B
Nacka
Sweden

**8. PERFORMING ORGANIZATION REPORT NUMBER**

N/A

**9. SPONSORING/MONITORING AGENCY NAME(S) AND ADDRESS(ES)**

EOARD
PSC 821 BOX 14
FPO AE 09421-0014

**10. SPONSOR/MONITOR'S ACRONYM(S)**

**11. SPONSOR/MONITOR'S REPORT NUMBER(S)**
Grant 07-3059

**12. DISTRIBUTION/AVAILABILITY STATEMENT**

Approved for public release; distribution is unlimited.

**13. SUPPLEMENTARY NOTES**

**14. ABSTRACT**

This is a final report for EOARD grant FA8655-07-1-3059 entitled "Improvement of electromagnetic code for phased array antenna design".
An existing time domain code for electromagnetic design and analysis of phased array antennas and other periodic structures such as frequency selective surfaces and meta-materials has been improved in several ways. The code which is named PBFDTD (Periodic Boundary FDTD) now handles magnetic materials (lossy and loss-free). Frequency domain surface currents and the electromagnetic field in the computational volume can be visualized. It is now also possible to use the code without the GUI, which for example makes it easier to couple it to stand-alone optimizers. That required, among others, new formats of the input and output files.
Several minor improvements of the code have also been done. For example lumped elements in the form of resistors, inductances and capacitances can now be modeled.

**15. SUBJECT TERMS**
EOARD, Radiofrequency radiation, Electromagnetics, Antennas

| 16. SECURITY CLASSIFICATION OF: | | | 17. LIMITATION OF ABSTRACT | 18, NUMBER OF PAGES | 19a. NAME OF RESPONSIBLE PERSON |
|---|---|---|---|---|---|
| a. REPORT | b. ABSTRACT | c. THIS PAGE | | | GEORGE W YORK, Lt Col, USAF |
| UNCLAS | UNCLAS | UNCLAS | UL | 14 | **19b. TELEPHONE NUMBER** *(Include area code)* +44 (0)20 7514 4354 |

**Table of Contents**

**Table of figures**

# 1 SUMMARY

This is a final report for EOARD grant FA8655-07-1-3059 entitled “Improvement of electromagnetic code for phased array antenna design”.

An existing time domain code for electromagnetic design and analysis of phased array antennas and other periodic structures such as frequency selective surfaces and meta-materials has been improved in several ways. The code which is named PBFDTD (Periodic Boundary FDTD) now handles magnetic materials (lossy and loss-free). Frequency domain surface currents and the electromagnetic field in the computational volume can be visualized. It is now also possible to use the code without the GUI, which for example makes it easier to couple it to stand-alone optimizers. That required, among others, new formats of the input and output files.

Several minor improvements of the code have also been done. For example lumped elements in the form of resistors, inductances and capacitances can now be modeled.

# 2 INTRODUCTION

Bellow follows the abstract and the statement for work of the proposal that earlier was submitted to EOARD.

## 2.1 Abstract of proposed research effort (submitted to EAORD)

For some years ago and also recently, EOARD has supported the development of a time domain computer code for phased array analysis and design under contract no. F61775-00-WE037 (Henrik Holter, Royal Institute of Technology, Stockholm, Sweden) and FA8655-05-01-3054 (Henrik Holter, private researcher). The code can also be used for frequency selective surface and radar cross-section calculations. The code, which is based on Dr. Henrik Holter's PhD thesis, is a unique concept. It is numerically highly efficient and has proved as quite useful at the AFRL, Hanscom, MA. Present commercial electromagnetic codes do not offer a comparable computational capability for wideband analysis of periodic structures.

The proposed work is made up of three different parts as presented below.

The main part of the code is today written in Fortran. A GUI developed in MATLAB is used for pre- and post-processing. The Fortran program and the GUI are today strongly linked. For some problems, for example optimization problems, where a large number of simulations need to be run it is most desirable to run the Fortran code directly without the GUI. The first proposed work is therefore to make that possible by removing the strong connection between the Fortran program and the GUI.

Knowledge of the surface currents on antennas and other structures are important for the physical understanding. The second part of the proposed work is therefore to extend the code so that surface currents on metal objects can be visualized.

The code can today handle dielectric materials and perfect electric conductors, but it cannot handle magnetic materials. The third proposed work is therefore to extend the code so it also will be able to handle magnetic materials. That would make the code even more useful.

## 2.2 Statement of work (submitted to EAORD)

The proposed service is divided into three parts.

### 2.2.1 Part 1

Remove the connection between the Fortran program and the GUI developed in MATLAB. The estimation is that this part constitutes 50% of the total work.

- The format of most of the input and output files will be changed. It will be easier than it is today to create the input files and to interpret the many output files.
- The GUI will be modified so it can handle the new formats of the input and output files.
- Some of the pre- and post-processing tasks that today are done with MATLAB must instead be integrated into the Fortran main program.
- The manual will be updated.

### 2.2.2 Part 2

Calculation and visualization of surface currents on metal object. The estimation is that this part constitutes 30% of the total work.

- The surface current will be calculated at frequencies specified by the user.
- The GUI will be modified so it can create surface current plots.
- The manual will be updated.

### 2.2.3 Part 3

Extend the code so it can handle magnetic materials. The estimation is that this part constitutes 20% of the total work.

- The user should be able to specify an arbitrary permeability of each material used.
- The GUI will be modified so it can handle this.
- The manual will be updated.

### 2.2.4 Deliverables

- Computer code, inclusive source code (FORTRAN and MATLAB GUI)
- Updated manual

## 3 METHODS, ASSUMPTIONS, AND PROCEDURES

The statement of work was presented in the previous section. The work that actually has been carried out is presented in this section.

All three parts in the statement of work have been completed. A presentation of the work follows below. In addition to the statement work, the following improvements of the code have been made.

1. An optimizer based on a genetic algorithm coupled to the software package has earlier been developed. This optimizer has been improved considerable during the current project. It is now easier to model advanced geometries. The optimizer does not longer use the GUI, which was the case in earlier versions. A result of that is that windows are no longer opened and closed during the optimization process. Also, the main program now runs without the status

windows popping up (when the genetic algorithm is used). All this means that both the optimizer and the main program are running in the background.

2. Lumped elements in the form of parallel RLC-circuits have been implemented into the code. Not all of the components in the parallel RLC-circuit need to be used, which means that the following parallel circuits can be modeled: R, L, C, RL, RC, LC and RLC.
3. Statement of work, part 2, surface current visualization. Not only the surface current can be visualized. Frequency domain E- and H-field in the computation volume can also be visualized. Several different plots of the currents and the fields can be generated.
4. The appearance of the GUI has been changed a little.
5. A status window is shown during a calculation. One thing presented in the status window is the convergence of the calculation. The way the convergence is calculated has been improved.

The manual for the software has been updated with the new features. It is recommended to read those parts before using the new features. For example, for the frequency domain field visualization, averaging of the time domain field components is used before the DFT is applied. The reason and the consequence of this are explained in the manual.

## 3.1 Statement of work, part 1

### 3.1.1 New format of input files

All information needed for a singe computation is stored in a text-file that normally is automatically generated by the GUI. The text-file contains both parameter settings and the geometry. If for example an optimizer is coupled to the main program, one must create the text file manually. This was earlier complicated because of the difficult and not documented format of the input file. The format of the input file has therefore been changed and documented. It is now easy to create the input file manually or by any other means.

The new format of the input file is explained in the manual and is therefore not described here.

### 3.1.2 New format of output files

After a computation has been performed, one to several output files with simulation data are generated. The exact number of output files depends on the settings in the input text file. The format of the output files was earlier not documented. The reason for that was that the user earlier always accessed the output files through the GUI.

The format of the output files is now documented (see the manual). Accessing the output files directly without using the GUI is usually only of interest if the software is used without the GUI. This may be the case, as mentioned above, if for example an optimizer is coupled to the code.

### 3.1.3 Running the software without the GUI

The software can now be used without the GUI. The steps needed for that are explained in the manual. As explained in the manual, a short executable MATLAB

script exists in the folder where the software is installed that contains those steps. The user can easily modify the script.

Earlier when the main program was running, a little status window was shown during the simulation. It is now possible to run the main program without this status window. This is for example used for the new genetic algorithm.

## 3.2 Statement of work, part 2

### 3.2.1 Calculation and visualization of surface currents on metal object

Frequency domain surface currents can be plotted on PEC surfaces and wires. Before the computation starts, the user specifies at what frequencies the surface currents shall be calculated.

The time domain unit cell technique used in cose is based on a unit cell that moves over the array face when the array is scanned to of broadside angles. The currents will however be plotted for one single stationary unit cell that not is moving. This is what the user would like to see.

### 3.2.2 3D-plots

The surface current can be visualized in the form of 3D-plots as shown in Figure 1. The quantity plotted in 3D-plots is the magnitude of the complex surface current. The surface, $J_s$, current is calculated from the H-field, $J_s=n\times H$, where n is the normal component to the surface.

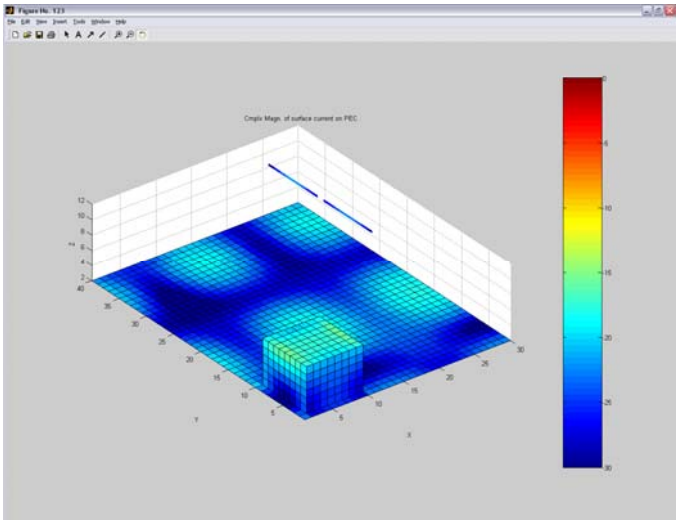

**Figure 1. Surface currents on PEC surfaces and wires.**

Creating 3D-plots of the surface current like the one above require a lot of computer resources (time and memory), which makes it difficult to plot surface currents on large structures. 2D-plots are then a better alternative.

### 3.2.3 2D-plots

2D-plots on planes through the computation volume can be generated. Not only the surface currents can be plotted on those planes, also the E- and H-field can be plotted.

The surface current on the plane is calculated from the H-field ($J_s=n\times H$) and it is calculated on the whole 2D-plane regardless of if there is PEC-material or not.

A GUI has been developed in order to facilitate the plotting. Through the GUI, the user can specify

- Frequency.
- 2D-plot plane (xy, yz or xz).
- Field quantity (Surface current, E- or H-field).
- Field components to use (x, y, z, x+y, y+z, z+x or x+y+z).
- Plot type: complex magnitude, magnitude or vector plot.
- Phase (for plot types magnitude and vector plot).
- Phase animation. Animations can be saved as .avi-files.
- Scaling: linear or logarithmic.

The frequency domain data is calculated by a DFT at the same time the FDTD computation is performed, “running DFT”. This require a lot of computer memory since six complex field components (3 E- and 3 H- components) must be saved for each FDTD-cell at each frequency specified by the user. This will also slow down the computation to some degree. All important parts in the main program has earlier been parallelized in order to take into account up to three CPU:s. The new implementation of the DFT for the field components has also been parallelized. In order to save memory and to reduce the calculation time, the user can specify a volume, less than the computational volume, wherein the frequency domain data is calculated.

The figures below show some examples of 2D-plots that can be generated.

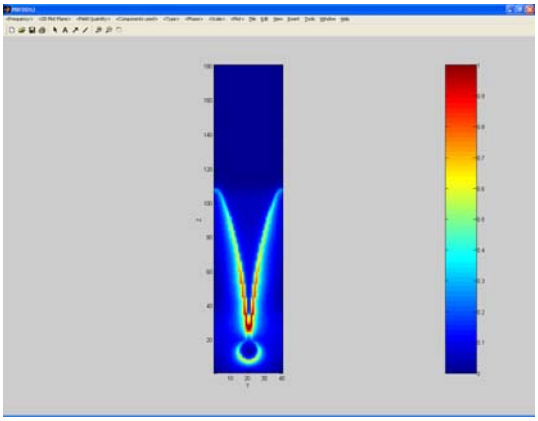

**Figure 2. Surface current on Vivaldi-element. Complex magnitude. Observe that the surface current is plotted on the whole 2D-plane and not only on PEC-surfaces. This is also mentioned above.**

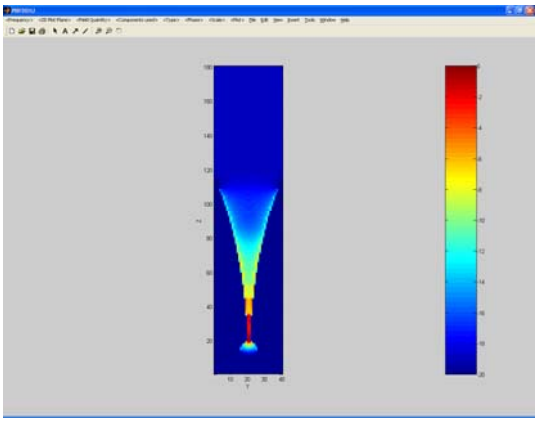

**Figure 3. Tangential E-field on Vivaldi-element. Complex magnitude.**

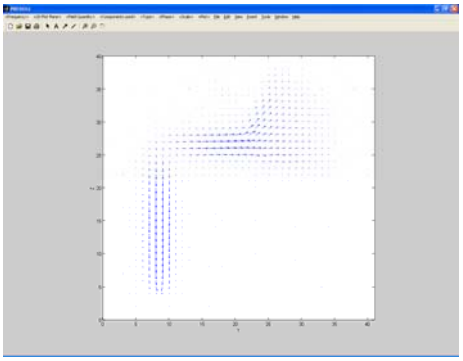

**Figure 4. Surface current on stripline feed for Vivaldi-element. Vector plot (the phase can be changed). As explained above, the surface current is calculated on the whole 2D-plane and not only on the stripline.**

## 3.3 Statement of work, part 3

Magnetic materials have been implemented. The user can now for each material used specify

- Relative permittivity
- Electric conductivity.
- Relative permeability.
- Magnetic conductivity.

### 3.3.1 A comment on the implementation of electric and magnetic materials

The FDTD-mesh is made up of a large number of small FDTD cells with size $\Delta x \times \Delta y \times \Delta z$. Two meshes are actually used in FDTD, one mesh for the E-field components and one mesh for the H-field components. The two meshed are displaced from each other by a distances $\Delta x/2$, $\Delta y/2$ and $\Delta z/2$ in the x-, y- and z-directions. The E- and H-field components are located in an FDTD-cell as shown in the figure below.

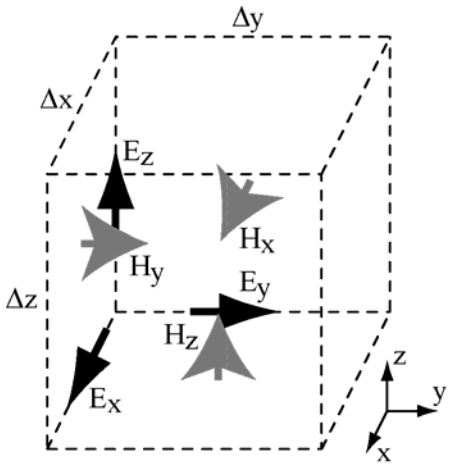


**Figure 5. FDTD-cell. Location of E- and H-field components.**

When materials are modeled in FDTD then electric materials are associated with the E-field components and magnetic materials are associated with the H-field components. Electric and magnetic materials are therefore not located at the same points within an FDTD-cell. This is not a problem but the user should understand what it means.

When an object is modeled then the surfaces of the object are always parallel to tangential E-field components. A consequence of that is that H-field components located on the surfaces are always directed in the direction normal to the surface. See the figure below and also see the FDTD-cell above. One should have this in mind when modeling objects. Below is an example where the reflection coefficient from two infinite radomes is calculated. One radome has an electric material and the other radome has a magnetic material.

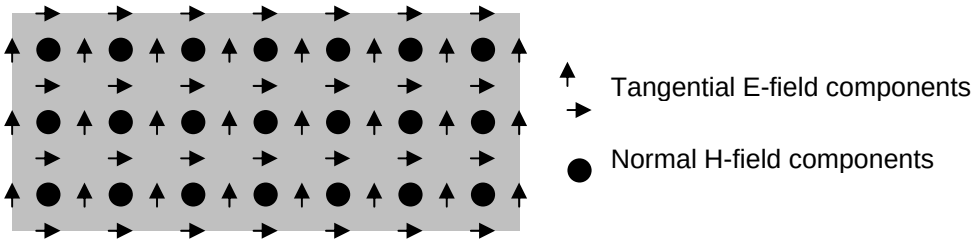


**Figure 6. E- and H-field components on the surface of an object.**

### 3.3.2 Example

A one layer radome with a thickness of about $\lambda_{material}/2$ at 3 GHz has been modeled with unit cell analysis, see Figure 7. The material in the radome is homogeneous. Two different materials have been used for the radome (two calculations have been performed), an electric material with $\varepsilon_r=4.0$ and a magnetic material with $\mu_r=4.0$. Averaging has been used for the material at the surfaces. This means that $\varepsilon_r=\mu_r==(4.0+1.0)/2=2.5$ at the surfaces.

The resolution used for the computation is 40 FDTD-cells/wavelength at the frequency 3 GHz.

The magnitude of the reflection coefficient for a radome with the electric material and for a radome with the magnetic material should be the same. Calculated reflection coefficients for the two radomes are shown in Figure 8 for normal incidence. The two

curves in the figure almost overlap. The small difference between the curves has to do with the implementation of electric and magnetic materials as has been discussed above.

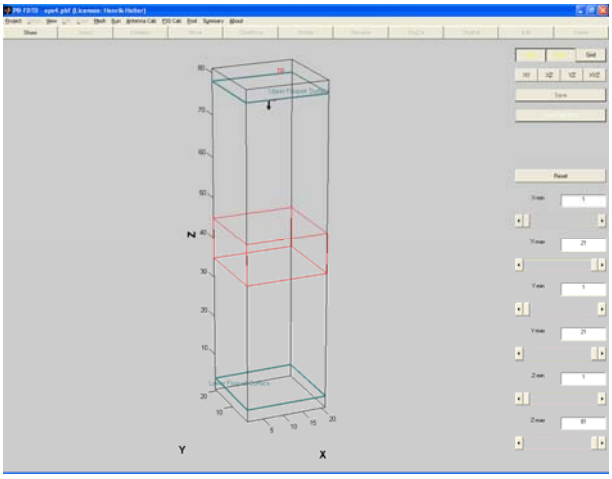

**Figure 7. Radome. Thickness about λ/2 at 3 GHz.**

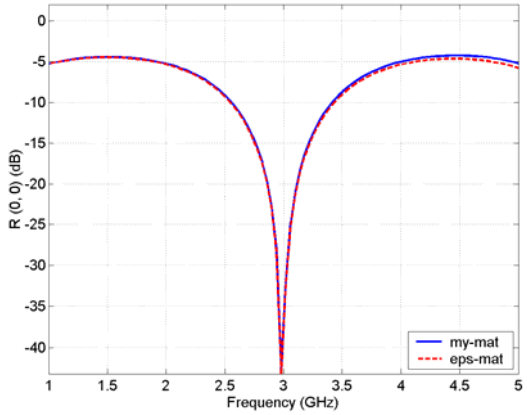


**Figure 8. Reflection coefficient. Zero order Floquet mode. Averaging has been used for the material at the two surfaces.**

As a comparison, averaging of the material at the surfaces in not used in Figure 9. Averaging can obvious be important! The radome with an electric material is more affected than the radome with a magnetic material in Figure 9. This is expected since the polarization of the plane wave used is parallel to the surface and the electric material has tangential components parallel at the surface, which not is the case for the magnetic material. This means that the modeling of the material at the surface is more important for electric materials for this particular example. When averaging not is used for the electric material then the radome will be electrical thicker, which lower the frequency where the reflection coefficient is low. This is exactly what can be observed in Figure 9.

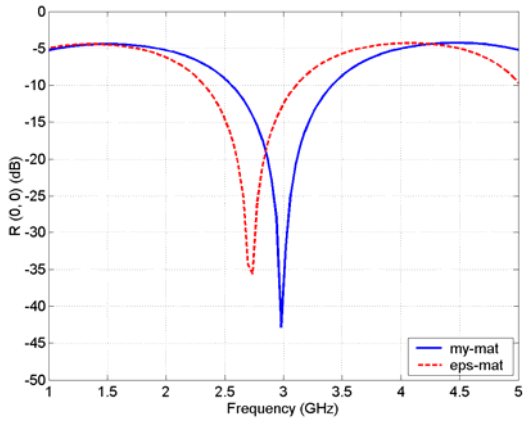


**Figure 9. Reflection coefficient. Zero order Floquet mode. Averaging has not been used for the material at the two surface.**

## 3.4 RLC-circuit

Lumped elements in the form of parallel RLC-circuits have been implemented. Not all of the components in the RLC-circuit must be used.

As an example, the reflection coefficient of a 2-wire transmission line terminated in an RLC-circuit with R=188 Ohm (equal to the characteristic impedance of the transmission line), L=1e-9 H and C=1e-12 F has been calculated, see the figure below. For comparison the exact reflection coefficient has also been calculated. The agreement between the two curves is very good.

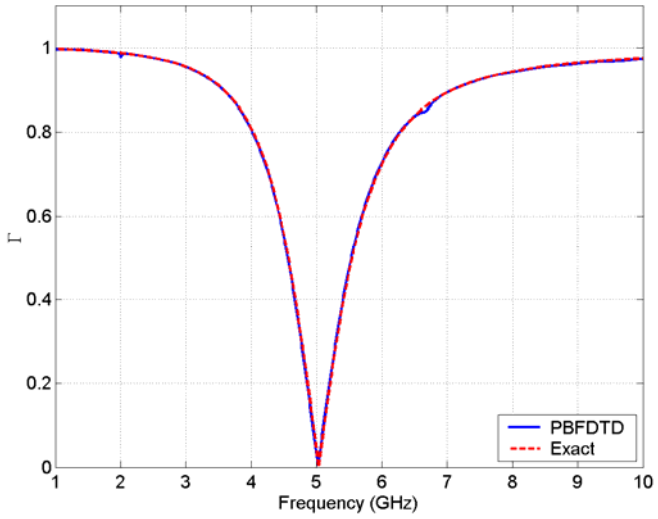


**Figure 10. Reflection coefficient. 2-wire transmission line terminated in a parallel RLC-circuit.**

## 4 CONCLUSIONS

All parts in the statement of work for the research project have been fulfilled. In addition to that, the code has also been improved in several other ways.

The new functions that have been implemented in the code during the EOARD funded research project have increased the codes usability considerable. It is now more up-to-date to handle the latest research problems within the areas phased array antennas, frequency selective surfaces and meta-materials.